Title
REACTIONS and WETTING BEHAVIOR IN THE MOLTEN ALUMINUM-FUSED SILICA SYSTEM

Author
Marumo, Chisato.

Publication Date
1975-08-01

REACTIONS AND WETTING BEHAVIOR IN THE MOLTEN ALUMINUM-FUSED SILICA SYSTEM

Chisato Marumo
(M. S. thesis)

August 1975

Prepared for the U. S. Energy Research and
Development Administration under Contract W-7405-ENG-48

DISCLAIMER

REACTIONS AND WETTING BEHAVIOR IN THE
MOLTEN ALUMINUM-FUSED SILICA SYSTEM

Table of Contents

REACTIONS AND WETTING BEHAVIOR IN THE MOLTEN ALUMINUM-FUSED SILICA SYSTEM

Chisato Marumo

Inorganic Materials Research Division, Lawrence Berkeley Laboratory
and Department of Materials Science and Engineering,
College of Engineering; University of California,
Berkeley, California 94720

ABSTRACT

The sessile drop technique was used to study the wetting behavior of fused silica by molten aluminum in the temperature range 800°C to 1000°C, and provided the specimens for the reaction studies.

Contact angle between fused silica and molten aluminum decreased down to 90° mainly due to the contribution of the free energy of the reaction $(-)\Delta g$ to the solid-liquid interfacial tension $\gamma_{s\ell}$ and due to the change of the surface tension $\gamma_{\ell v}$ of molten aluminum which dissolves silicon as a result of the reaction. Below 90° the periphery of the drop was in contact with the intermediate reaction layer.

Three reaction layers, I (adjoining the drop), II, III (adjoining SiO_2) were formed. The main reaction layer I-b at 800°C is identical to layer I-a at 900°C; and the thin layer at 800°C is identical to layers II-a and III-a at 900°C. Using an Al drop saturated with Si at 800°C, two reaction layers II-c and III-c were formed; a layer equivalent to I-a and I-b was not present.

Possible reaction mechanisms between Al and SiO_2 are proposed. At the test temperature layer I is assumed to be AlO which is stabilized by forming a solid solution with SiO and Al_2O, and layer III is assumed to form a spinel type structure $(XAlO(1-x)SiO)Al_2O_3$ which is also stabilized by solid solution. Reactions then proceed by counterdiffusion

of Al ions and Si ions through the reaction layers. At room temperature the reaction products dissociate to form crystalline Al_2O_3, Al and Si.

I. INTRODUCTION

Reactions and wetting behavior in ceramic-metal systems are of technological interest as well as scientific interest in a number of fields. In the fields of cermets and composites, reactions and wetting at ceramic-metal interfaces are of critical importance in determining the properties of the fabricated materials. In the field of electronics, metals are used in contact with ceramics in integrated microcircuits. With a potentially reactive system, devices may become degraded as a result of ceramic-metal reactions.

The degree of wetting of a solid by a liquid in a solid-liquid-vapor system has been expressed by Young's equation under chemical stable and metastable equilibrium conditions. Aksay, Hoge and Pask[1] treated the thermodynamics of wetting in a solid-liquid-vapor system by considering the conditions that minimize the total free energy of the system. They also extended their theory to non-equilibrium conditions. They showed that an interfacial reaction resulted in the lowering of the solid-liquid interfacial tension by the free energy of the reaction which could result in the spreading of a liquid drop on a solid substrate.

Reactions between aluminum and silica are thermodynamically favorable. Although the following formulation has been proposed,[2]

$$4\ Al + 3SiO_2 \rightarrow 2Al_2O_3 + 3Si \qquad (1)$$

there is a possibility that Al^{+}, Al^{++} and Si^{++} may have important roles during the course of the reactions as long as some aluminum remains that

is not fully oxidized. This possibility is related to the conditions under which the stabilities of suboxides of aluminum and silicon can be realized. To determine the reaction mechanism, a detailed analysis of the compositions and microstructures of the reaction layers is considered to be necessary.

The objectives of this research is to understand the mechanism of reaction between molten aluminum and fused silica, and to study the effect of the interfacial reaction on wetting behavior.

II. THEORY AND LITERATURE SURVEY

A. Theory of Wetting

1. Theory of Wetting Under Chemical Equilibrium Conditions

Young's equation has been used to express the relationship between the contact angle of a liquid on a solid and the three interfacial tensions in a solid-liquid-vapor system under chemical equilibrium conditions:

$$\gamma_{sv} - \gamma_{s\ell} = \gamma_{\ell v} \cos \theta \tag{2}$$

where γ is the interfacial tension between solid-vapor (sv), solid-liquid ($s\ell$) and liquid-vapor (ℓv) phases. Contact angle θ is measured through the liquid phase as shown in Fig. 1.

Johnson[3] derived Young's equation from the thermodynamics of a solid-liquid-vapor system using the method of Gibbs. Aksay, Hoge and Pask[1] extended Johnson's treatment of the thermodynamics of wetting by considering the conditions to minimize the total free energy in the system under chemical equilibrium and non-equilibrium conditions.

The total free energy change of a multicomponent system can be expressed as

$$dG = \left(\frac{\partial G}{\partial T}\right)dT + \left(\frac{\partial G}{\partial P}\right)dP + \left(\frac{\partial G}{\partial A}\right)dA + \sum_i \left(\frac{\partial G}{\partial n_i}\right) dn_i$$

$$= - SdT + VdP + \gamma dA + \sum_i \mu_i dn_i \tag{3}$$

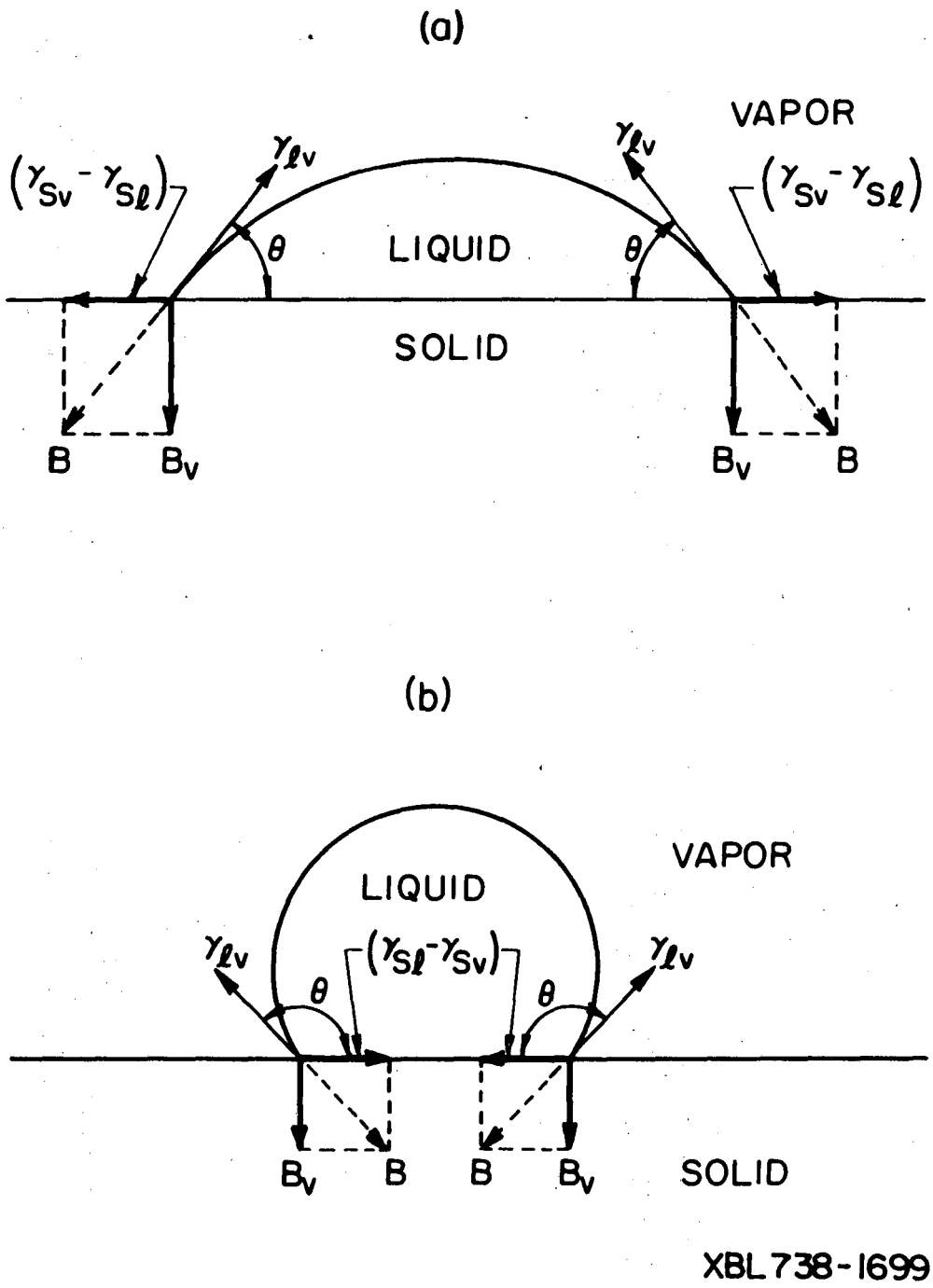

Fig. 1. Balance of forces acting at the solid-liquid-vapor contact for an (a) acute contact angle, and (b) obtuse contact angle.[1]

The chemical potential of the ith component, μ_i, surface tension γ, and specific surface free energy g of a multicomponent system are related by

$$\mu_i = \bar{G}_i = \left(\frac{\partial G}{\partial n_i}\right) n_j,\ P,\ T. \tag{4}$$

$$\gamma = \left(\frac{\partial G}{\partial A}\right)_{T,P,V,n_i} \tag{5}$$

$$g = (G - G^{\alpha} - G^{\beta})/A. \tag{6}$$

γ and g are related as

$$g = \gamma + \sum_i \Gamma_i \mu_i \tag{7}$$

where $\Gamma_i = \frac{n_i^{\alpha\beta}}{A}$, the surface concentration in units of moles per unit area.

The total differential of the free energy of a solid-liquid-vapor system at constant temperature and pressure is

$$dG = \sum_i \mu_i^s\, dn_i^s + \sum_i \mu_i^l\, dn_i^l + \sum_i \mu_i^v\, dn_i^v + \gamma_{s\ell} dA_{s\ell} + \gamma_{sv} dA_{sv} + \gamma_{\ell v} dA_{\ell v}$$

$$+ \sum_{\alpha\beta} \left\{ \sum_i \left(\frac{\partial G^{\alpha\beta}}{\partial n_i^{\alpha}}\right) dn_i^{\alpha} + \sum_i \left(\frac{\partial G^{\alpha\beta}}{\partial n_i^{\beta}}\right) dn_i^{\beta} + \sum_i \left(\frac{\partial G}{\partial n_i^{\alpha\beta}}\right) dn_i^{\alpha\beta} \right\} \tag{8}$$

where $\sum_{\alpha\beta}$ is taken over all three interfaces. The properties of interfaces depend not only on variables of the interface, but also on the

variables of the adjacent bulk phases. At total thermodynamic equilibrium, dG = 0. Since the variations of mass are independent of the variations of area,

$$\gamma_{s\ell} dA_{s\ell} + \gamma_{sv} dA_{sv} + \gamma_{\ell v} dA_{\ell v} = 0 \tag{9}$$

and

$$\sum_i \mu_i^s dn_i^s + \sum_i \mu_i^l dn_i^l + \sum_i \mu_i^v dn_i^v$$

$$+ \sum_{\alpha\beta} \left\{ \sum_i \left(\frac{\partial G}{\partial n_i^\alpha} \right) dn_i^\alpha + \sum_i \left(\frac{\partial G^{\alpha\beta}}{\partial n_i^\beta} \right) dn_i^\beta + \sum_i \left(\frac{\partial G^{\alpha\beta}}{\partial n_i^{\alpha\beta}} \right) dn_i^{\alpha\beta} \right\} = 0 \tag{10}$$

At chemical equilibrium Eq. (10) is satisfied and has a static value. If a drop is placed on a flat and rigid solid surface, a solid-liquid interface will form if

$$\delta G = \delta \int_{s\ell} \gamma_{s\ell} dA_{s\ell} + \delta \int_{sv} \gamma_{sv} dA_{sv} + \delta \int_{\ell v} \gamma_{\ell v} dA_{\ell v} < 0 \tag{11}$$

Thus, the free energy changes for the non-reactive system are only associated with changes in the interfacial areas; the equilibrium condition corresponds to the case when $\delta G = 0$.

2. Theory of Wetting Under Chemical Non-equilibrium Conditions

Under chemical non-equilibrium conditions, the effect of any chemical reaction on the interfacial tension has to be considered. It has been reported that interfacial reactions such as oxide formation at the solid-liquid interface and solution of a component of the liquid by

the solid result in the increase of the wettability of the solid by the liquid.

Aksay et al.[1] extended the treatment of thermodynamics of wetting to non-equilibrium conditions considering the contribution of the free energy of the interfacial reaction.

Under chemical non-equilibrium conditions, Eq. (10) is not satisfied and the phases of the solid-liquid-vapor system will react with each other through the interface to achieve a chemical equilibrium. Mass transfer across the interface must result in a net decrease of the free energy of the system at any time.

At the first instance of formation of an interface, only the interfacial region is involved in the chemical reaction, and the corresponding initial decrease in the free energy of the system is totally attributed to the decrease in the free energy of the interfacial region. The magnitude of the decrease in the specific interfacial free energy, $(-)\Delta g$, then is directly equal to $(-\Delta G^{\alpha\beta}/A)$. The corresponding interfacial tension is similarly reduced by an amount $(-)\Delta g^{\alpha\beta}$

$$\gamma_{\alpha\beta} = g^{\alpha\beta} - \sum_i \mu_i \Gamma_i^{\alpha\beta} \qquad (12)$$

as schematically shown in Fig. 2. If this addition to the driving force for wetting $(\gamma_{sv} - (\gamma_{s\ell} + \Delta g^{\alpha\beta}))$ results in a value that exceeds $\gamma_{\ell v}$, spreading will occur.

Diffusion of a component into the bulk phases after the reaction at the interface decreases the chemical potential gradient from the interface to bulk phases. This reduces the driving force for the

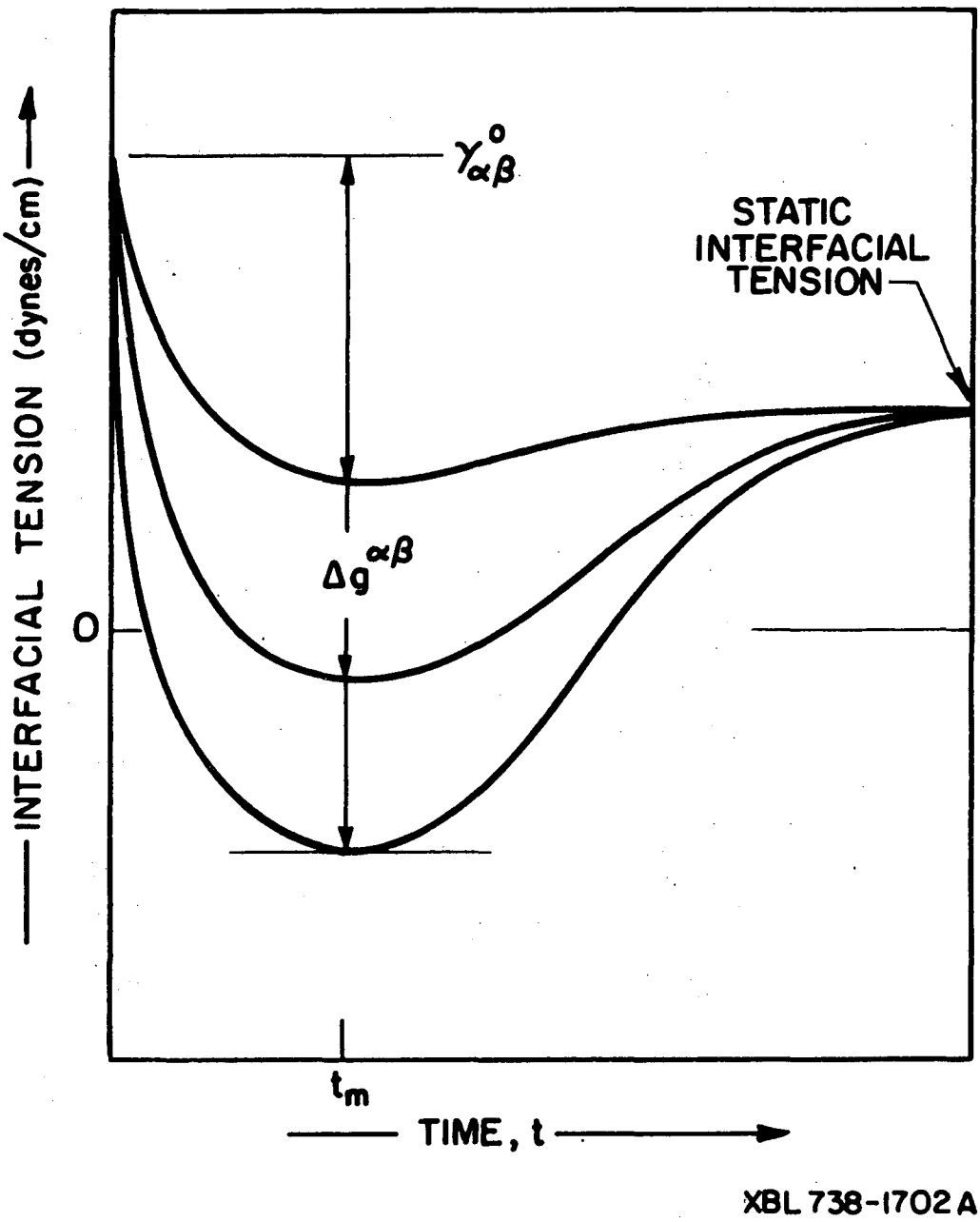

Fig. 2. Change of dynamic interfacial tension with time during a chemical reaction between two phases. The magnitude of reduction of the interfacial tension at t_m is proportional to $\Delta g^{d\beta}$.

reaction and $\gamma_{\alpha\beta}$ increases toward the static interfacial tension of the reacted bulk phases. If the interfacial energy reduction at the solid-liquid interface is large enough and also if the diffusion rates of the reaction components in the bulk phase are slow enough relative to the flow rate of the liquid, the liquid at the periphery of the drop will remain in contact with the unreacted solid and the liquid drop will spread on the solid substrate.

B. Reaction Studies in the Al-SiO_2 System

Chemical reaction between aluminum and silica was observed by Brondyke[4] in a study of the effect of molten aluminum on silica refractories which had porosities of 3-30%. Considerable reactions between the refractories and molten aluminum were observed at 700°C to 900°C.

Cratchley and Baker[5] observed a solid state chemical reaction in an etched section of silica fiber reinforced aluminum at 500°C. They reported that the strength of the composite began to decrease at 400°C and that the effect was probably due to a chemical reaction between silica and aluminum.

Standage and Gani[2] studied the chemical reaction between Al and SiO_2 by dipping fused silica rods into molten aluminum in air at 660° to 800°C. They detected Si and η-, θ-, α - Al_2O_3 as reaction products. Although they did not analyze the composition in the reaction layer in detail, their X-ray fluorescence micrograph of the reaction layer did not show any concentration gradients of Al and Si. They also studied the effects of the addition of Bi and Sb on the Al-SiO_2 reaction. They proposed that a complex interfacial layer formed by the absorbed water

and alloying elements with silica affected the dwell or incubation time of the reaction and the following reaction kinetics. Although they suggested that at low concentrations of Bi and Sb diffusion was not rate controlling and that at higher concentrations of Bi and Sb diffusion might be rate controlling, it seems unlikely that the basic reaction mechanism could be changed by the addition of Bi or Sb up to 2.5 wt%, the composition range they studied.

Prabriputaloong and Piggott[6] studied the Al-SiO_2 reaction in a manner similar to that used by Standage and Gani but in vacuum. They observed that the dwell time was drastically reduced under vacuum as compared to air. They suggested that the presence of Al_2O_3 film on the surface of molten aluminum in air caused the increased dwell time of the reaction and denied the existence of complex interfacial layers proposed by Standage and Gani.

Prabriputaloong and Piggott[7,8] also studied the reaction between an Al thin film and SiO_2 plate. Solid state reactions took place as low as 400°C. The reaction products observed are θ- and α-Al_2O_3 and Si below the melting point of Al. Above the melting point of Al, they indicated the formation of a volatile oxide of aluminum and only Si was detected as a reaction product. The literature search thus indicates that the mechanism of the Al-SiO_2 reaction is not yet well understood.

C. Stability of Oxides of Aluminum and Silicon

A knowledge of the stability of suboxides of Al and Si is required to understand the reaction between Al and SiO_2 since it is redox in nature. Especially, the question of whether suboxides of Al and Si could exist independently or in solid solution in the solid state is

decisive in the understanding of the reaction mechanism.

1. Aluminum Oxides

The existence of gaseous aluminum suboxides, Al_2O and AlO, is well established. In the vapor pressure study of the aluminum-oxygen system, Brewer and Searcy[9] showed that under reducing conditions, Al_2O_3 vaporized to Al, O, AlO and Al_2O with AlO as the major aluminum oxide species. In the presence of aluminum metal, the volatility of Al_2O_3 was much increased, a result which was attributed to the formation of gaseous Al_2O.

The existence of the suboxides of aluminum in the solid state has been discussed by several authors. Baur and Brunner[10] observed a melting point maximum (2046°C) at 15 wt% Al in the Al-Al_2O_3 mixture in a carbon crucible. They attributed this maximum to a compound Al_8O_9. Kohlmeyer and Lundquist[11] suggested that the maximum melting point was due to the compound AlO rather than Al_8O_9. Since the samples were heated in a graphite crucible in these experiments, the possibility of contamination by carbon should be considered. Foster, Long and Hunter[12] studied the Al_2O_3-Al_4C_3 phase diagram. They suggested that the compound observed by Baur and Brunner and by Kohlmeyer and Lundquist was most probably Al_4O_4C. Yanagida and Kröger[13] who repeated the experiments done by Baur and Brunner observed a melting point maximum at 25 wt% Al. They attributed this phenomenon to the presence of the ternary system Al_2O_3-Al_4C_3-Al. The critical composition which corresponds to the maximum melting point was considered to be determined by kinetic factors, differing from case to case, depending on the exact condtiions of the experiments. This explains the difference of maximum melting point composition observed by Baur and Brunner (Al_8O_9, Al 15 wt%); by Kohlmeyer

and Lundquist (AlO, Al 21 wt%); and by Yanagida and Kröger (Al 25 wt%). Yanagida and Kröger heated the Al-Al_2O_3 mixture surrounded by Al_2O_3 powder with an outer crucible of molybdenum in an inert atmosphere and examined the microstructure of the quenched specimens to detect melting in the mixture. They concluded there was no significant change of the melting point of Al_2O_3 by the addition of Al, at least up to Al_2O_3-50 wt% Al.

Hoch and Johnson[14] claimed, from a high temperature X-ray diffraction study, that solid Al_2O and AlO were formed by heating the mixture of Al and Al_2O_3 above 1100°C. But later, Yanagida and Kröger attributed these to Al_4C_3 and $AlTaO_4$ which were formed due to the contamination of the sample. The results of high temperature X-ray diffraction of Al-Al_2O_3 mixture by Yanagida and Kröger showed several weak, broad peaks besides a set of peaks for α-Al_2O_3 between 660°C and 1700°C. They ascribed these weak peaks to molybdenum carbide, aluminum carbide and aluminum-molybdenum alloy, and they concluded that solid AlO was not formed.

Low energy electron diffraction (LEED) studies of the (001) surface of α-alumina have revealed a structural transformation upon heating in vacuum. The features of the structural transformation are summarized as follows:[15-17]

(1) Upon heating α-Al_2O_3 in a wide range of vacuum conditions, a diffraction pattern of the (001) surface corresponding to the bulk lattice arrangement ((1 x 1) structure) persists up to nearly 900°C. If the temperature is raised over 900°C for even a few minutes, the (001) surface begins to give rise to a complex diffraction pattern. More

prolonged heating at about 1000°C fully develops the corresponding structure (rotated ($\sqrt{31}$ x $\sqrt{31}$) structure).

(2) Vacuum conditions are not critical. At 1000°C, the structural transforamtion occurred equally readily at 5 x 10^{-10} torr, 10^{-6} torr and in pure oxygen at pressures as high as 3 x 10^{-4} torr.

(3) Heating the $\sqrt{31}$ structure in air at 1250°C for 10 min gave an even more intense bulk (1X1) pattern.

(4) When aluminum metal was condensed on the (001) alumina surface which exhibited the (1 x 1) surface structure, the transformation temperature to the $\sqrt{31}$ structure was slightly lowered.

(5) Silicon is known to etch alumina surfaces at low deposition rates without forming a deposit. Silicon evaporation onto the $\sqrt{31}$ structure surface at 800°C resulted in the recovery of the (1 x 1) structure, while silicon vapor etching above 900°C resulted in some enhancement of resolution and intensity of the $\sqrt{31}$ structure.

These experimental results indicate that at low partial pressures of oxygen and at high temperatures the surface has an oxygen deficient structure with respect to the bulk structure of alumina. It is evident from the fact that the recovery of the bulk pattern becomes more difficult after prolonged heating at temperatures above 1000°C, that the $\sqrt{31}$ structure should be ascribed to a definite surface phase rather than to a simple surface layer reconstruction. Charig[15] suggested that relocation of the Al atoms in tetrahedral sites as in γ-alumina (spinel type structure) instead of octahedral sites would be consistent with the formation of a surface layer containing AlO. Based on Charig's observation, Brennan and Pask[18] postulated that at temperatures above 900°C to

1000°C and at low pressures an oxygen deficient surface of some unknown thickness exists containing some AlO in a spinel-type structure. They also postulated that on cooling in vacuum this structure persists; however, on exposure to oxygen or moisture the distribution of cations remains essentially the same but the valence of Al^{++} increased to Al^{3+} resulting in γ-Al_2O_3. French and Somorjai[17] postulated that along with the change of chemical composition at high temperature, the aluminum cation, Al^{3+}, is reduced in the oxygen-deficient surface layer to Al^{+} or Al^{++}. They also suggested from the compositions and the properties of other oxides of group III and IV elements that if the $\sqrt{31}$ structure has a composition which corresponds to Al_2O (or AlO), it would be likely to form a cubic structure in which the cation is appreciably larger than in the underlying hexagonal (001) substrate. Strong mismatch due to the difference in structure and ion sizes in the two phases should be expected.

Yamaguchi[19] studied the oxidation of aluminum metal surface and presented electron diffraction patterns which provided evidence for the existence of aluminum suboxides between Al and Al_2O_3 on the aluminum metal surface oxidized at 300°C.

In conclusion, there has been no clear evidence to support the existence of solid aluminum suboxides as a bulk phase. But from the studies of alumina surfaces at high temperatures under high vacuum and from the oxidation studies of aluminum, the existence of an aluminum suboxide or an oxygen deficient alumina structure as a surface phase has been confirmed.

2. Silicon Oxides

The existence of gaseous SiO has been recognized by spectroscopic investigations.[20] A mixture of Si and SiO_2 is known to react and vaporize as SiO gas.[21] SiO_2 vaporizes under neutral conditions predominantly to SiO and O_2 gases.[22] Kubaschewski, Evans, and Alcock[23] reviewed the thermodynamic properties of SiO and estimated the thermodynamic quantities.

For the reaction:

$$Si(s) + 1/2\ O_2(g) = SiO(g) \qquad (13)$$

$$\Delta H^{\circ}_{298} = -\ 23{,}200 \pm 2{,}000\ \text{cal/mole}$$

The entropy of gaseous SiO is $S^{\circ}_{298} = 50.55 \pm 0.1$ e.u.

Solid SiO may be prepared in a metastable amorphous or poorly crystallized form by condensation of SiO gas upon a cold surface.[24] The metastable SiO solid prepared by quenching SiO gas begins to disproportionate to Si and SiO_2 at an appreciable rate around 400°C-700°C. Solid SiO is very similar in appearance to a mixture of Si and SiO_2 which often results if the quenching rate of SiO vapor is not rapid enough. The most characteristic property of solid SiO is an electron and X-ray diffraction ring corresponding to a d-spacing of 3.60 ± 0.05 Å. This solid is completely soluble in HF while a mixture of Si and SiO_2 dissolves only partially, leaving Si as a residue.

Stability of solid SiO at high temperatures has been discussed by a number of investigators. Gel'd and Kochev[25] claimed to have prepared

amorphous silicon monoxide by heating an intimate mixture of silica and silicon to 1250°C-1350°C. On the other hand, Schäfer and Hörnle,[21] Grube and Peidel,[26] and Von Wartenberg[27] reported that amorphous SiO is unstable at about 1000°-1150°C.

High temperature X-ray diffraction analysis of mixtures of Si and SiO_2 below 900°C by Brewer and Edwards[24] showed that all the diffraction lines could be attributed to Si, β-tridymite, and β-crystobalite. This proved that solid SiO is thermodynamically unstable and disproportionates to Si and SiO_2 below 900°C. Hoch and Johnston[28] presented evidence for an X-ray pattern of SiO at 1250°C to 1300°C, but Geller and Thurmond[29] pointed out that the organic cement used in the samples would form silicon carbide and that the observed X-ray pattern was similar to that expected for a mixture of SiC and β-cristobalite. Potter[30] reported that a mixture of Si and SiO_2 was not liquified at 1700°C, and Brewer and Edwards[24] confirmed a higher melting point for the Si-SiO_2 mixture than for either of its components.

Brewer and Greene[31] pointed out from thermodynamic considerations that if there is any stable temperature range of SiO, the lower limit of that range should be below the melting point of Si. They made a differential thermal analysis of a Si-SiO_2 mixture up to the melting point of Si and did not detect any evidence of the existence of stable SiO. They postulated that the higher melting point of a Si-SiO_2 mixture formerly reported by Brewer and Edwards may have been due to the partial reduction of SiO_2 to SiO_{2-x}.

Van Wartenberg[27] determined the heat of solution of SiO, Si and SiO_2 in a $AgClO_4$-HF solution. From his data, Brewer and Edwards showed that

$$1/2\ Si(S) + 1/2\ SiO_2\ (\text{cristobalite}) = SiO\ (\text{amorphous})$$

$$\Delta H^{o}_{298} = 0.0 \pm 1.5\ \text{kcal.} \qquad (14)$$

They also estimated the entropy of amorphous SiO as S = 7.3 e.u. at 298°K, which led to ΔS^{o}_{298} = - 0.05 ± 1.0 e.u. and ΔG^{o}_{298} = 0.0 ± 3.3 kcal for Eq. (14). The result is undecisive as far as stability at room temperature is concerned. At 1200°K, they estimated S - 23.3 e.u. for amorphous SiO. For Eq. (14)

$$\Delta S^{o} = 1.5 \pm 3.0\ \text{e.u.}$$

$$\Delta H^{o} = 1.0 \pm 3.0\ \text{kcal}$$

$$\Delta G^{o} = - 0.9 \pm 6.6\ \text{kcal}$$

The uncertainty is too large to allow any decisive conclusions from the thermodynamic data alone. However, it is noted that there is a definite trend toward increase in stability as temperature is increased.

As reviewed, there is no doubt about the existence of metastable amorphous SiO at room temperature which disproportionates on heating. Experimental evidence has not been consistent about the existence of stable solid SiO at high temperature, mainly because of experimental difficulties.

From available thermodynamic data in literature,[23,24,32] the standard free energies of possible reactions in the Al-SiO_2 system at 800°C were calculated and listed in Table I.

3. Compositions Containing Aluminum and Silicon Suboxides

It is significant that no reports have been made of studies of suboxides of aluminum or silicon in the presence of the other. Although AlO

Table I. Standard Free Energies of Reactions

No.	Reaction	$\Delta G^{o}_{800°C}$ (Kcal)
1.	$3/4\ Al(\ell) + O_2(g) = 2/3\ Al_2O_3(S)$	-213
2.	$4Al(\ell) + 3SiO_2(glass) = 2Al_2O_3(S) + 3Si(S)$	-149
3.	$4Al(\ell) + O_2(g) = 2Al_2O(g)$	-104
4.	$2Al(\ell) + O_2(g) = 2AlO(g)$	- 4
5.	$AlO(g) + Al(\ell) = Al_2O(g)$	- 50
6.	$2Al_2O(g) + O_2(g) = 4AlO(g)$	96
7.	$2Al(\ell) + SiO_2(glass) = Al_2O(g) + SiO(g)$	69
8.	$4Al(\ell) + SiO_2(glass) = 2Al_2O(g) + Si(S)$	59
9.	$Al(\ell) + SiO_2(glass) = AlO(g) + SiO(g)$	119
10.	$Al_2O(g) + SiO_2(glass) = 2AlO(g) + SiO(g)$	169
11.	$Al(\ell) + Al_2O_3(S) = 3AlO(g)$	314
12.	$4Al(\ell) + Al_2O_3(S) = 3Al_2O(g)$	163
13.	$2Si(S) + Al_2O_3(S) = Al_2O(g) + 2SiO(g)$	182
14.	$Si(S) + O_2(g) = SiO_2(glass)$	-164
15.	$SiO(g) + 1/2\ O_2(g) = SiO_2(glass)$	-121
16.	$2Si(S) + O_2(g) = 2SiO(g)$	- 86
17.	$Si(S) + SiO_2(glass) = 2SiO(g)$	78
18.	$2Al(\ell) + H_2O(g) = Al_2O(g) + H_2(g)$	- 7
19.	$Si(S) + H_2O(g) = SiO(g) + H_2(g)$	2

is unstable as a bulk phase, it could be possible that it is stabilized by forming a solid solution with SiO, since the free energy of the system could be reduced by the formation of a solid solution. Tressler, Moore and Grane[33] studied the reactions between titanium and alumina. They postulated the possibility of a substantial amount of Al ions, most likely Al^{++}, in the NaCl-type TiO phase on the basis of a larger unit cell than that for TiO.

Considering the presence of oxygen-deficient alumina surfaces under lower pressures, it is possible that spinel structures containing Al_2O_3 and AlO, particularly with SiO in solid solution, could form with certain conditions and compositions.

III. EXPERIMENTAL PROCEDURE

A. Materials and Specimen Preparation

The sessile drop technique was used to study wetting behavior and provided specimens for reaction studies at the interface. The aluminum* (99.999% pure) was obtained in the form of 1/4 in. diameter rods. The aluminum pieces were cut from these rods and ground into spheres so that on melting an advancing contact angle would be measured. These specimens weighed approximately 0.1g except for those used for X-ray diffraction study, which weighed approximately 1.0g. The fused silica** (>99.97%) used for substrates in the sessile drop experiments was obtained as a transparent optically polished plate 1/8 in. or 1/4 in. thick, which was cut into the form of 3/4 in. squares. Both the aluminum and silica specimens were cleaned ultrasonically in isopropyl alcohol for about 15 min. The aluminum piece was placed on a silica plaque in a Ta-foil resistance vacuum furnace.

B. Experimental Conditions

The experimental setup of the sessile-drop furnace is shown in Fig. 3. The Ta-foil tube was connected to water-cooled copper electrodes by copper holders. The fused silica plaques rested on the flat surface of an alumina "dee" tube which was fitted inside the Ta-foil tube. The total pressure of the furnace was always kept less than 3×10^{-5} torr during experiments. The temperature was measured with a Pt-Pt 10% Rh thermocouple placed inside of the "dee" tube. Contact angle measurements

---

* United Mineral & Chemical Corp., New York, N.Y.
**Thermal American Fused Quartz Co., Montville, N.J.

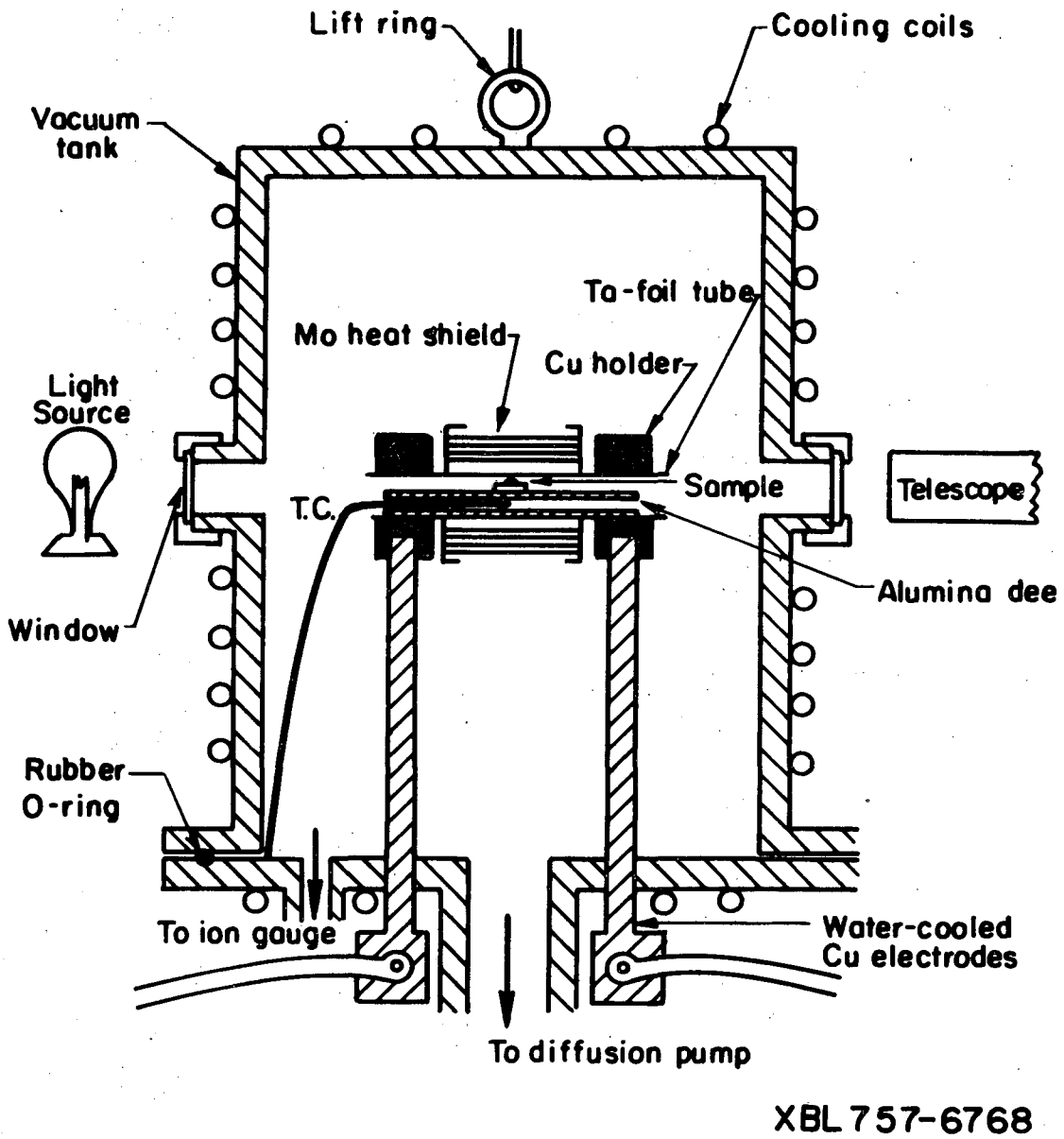

Fig. 3. Schematic diagram of sessile drop furnace.

were made over the temperature range 660°-1200°C through fused silica windows in the vacuum chamber with a telescope which was capable of measuring contact angles within ± 1°.

C. Analysis of the Experiments

After cooling down, the specimens were cut and polished to examine the interfacial region with an optical microscope and a scanning electron microscope. Compositions in the cross-section perpendicular to the Al-SiO_2 interface were determined by an electron microprobe. Line scanning of approximately 75 μm length was used to get the average composition in the inhomogeneous reaction layers. The reaction products were analyzed by X-ray diffraction.

IV. EXPERIMENTAL RESULTS

A. Sessile Drop Experiments of Molten Aluminum on Fused Silica

Reactions between Al and SiO_2 have been observed. In such a reactive system, precautions should be taken to assure the measurement of an advancing contact angle on melting of a piece of Al on a substrate. Examples of contact angle vs. time are shown in Fig. 4. Preliminary experiments at 800°C indicated that the contact angle measured using a spherical piece of Al changed smoothly, while the contact angle using a cubic piece of Al changed irregularly. Experiments using cubic pieces were inconsistent because of reactions prior to forming spherical drops on melting of Al. Spherical pieces of Al were thus used in this study to measure advancing contact angle since on melting the periphery of the Al drop comes in contact with initially unreacted SiO_2.

The temperature dependence of contact angle of molten aluminum on fused silica is shown in Fig. 5. The temperature was raised continuously at the rate of 10°C/min from the melting point of aluminum (660°C) to 1200°C. The reaction between Al and SiO_2 started immediately after melting of Al at 660°C. The dynamic contact angle decreased with temperature with an arrest at 90° in a temperature range around 900°C.

The contact angle at 800°C changed continuously until it reached 67° after approximately 50 minutes (Fig. 4). Until the contact angle reached approximately 90°, the periphery of the Al drop kept in contact with SiO_2 fresh surface; below 90°, the periphery of the drop was in contact with the reaction layer. During cooling, cracks appeared in the SiO_2 near the SiO_2-reaction layer boundary because of the large difference in coefficients of thermal expansion. Cross-sections of the

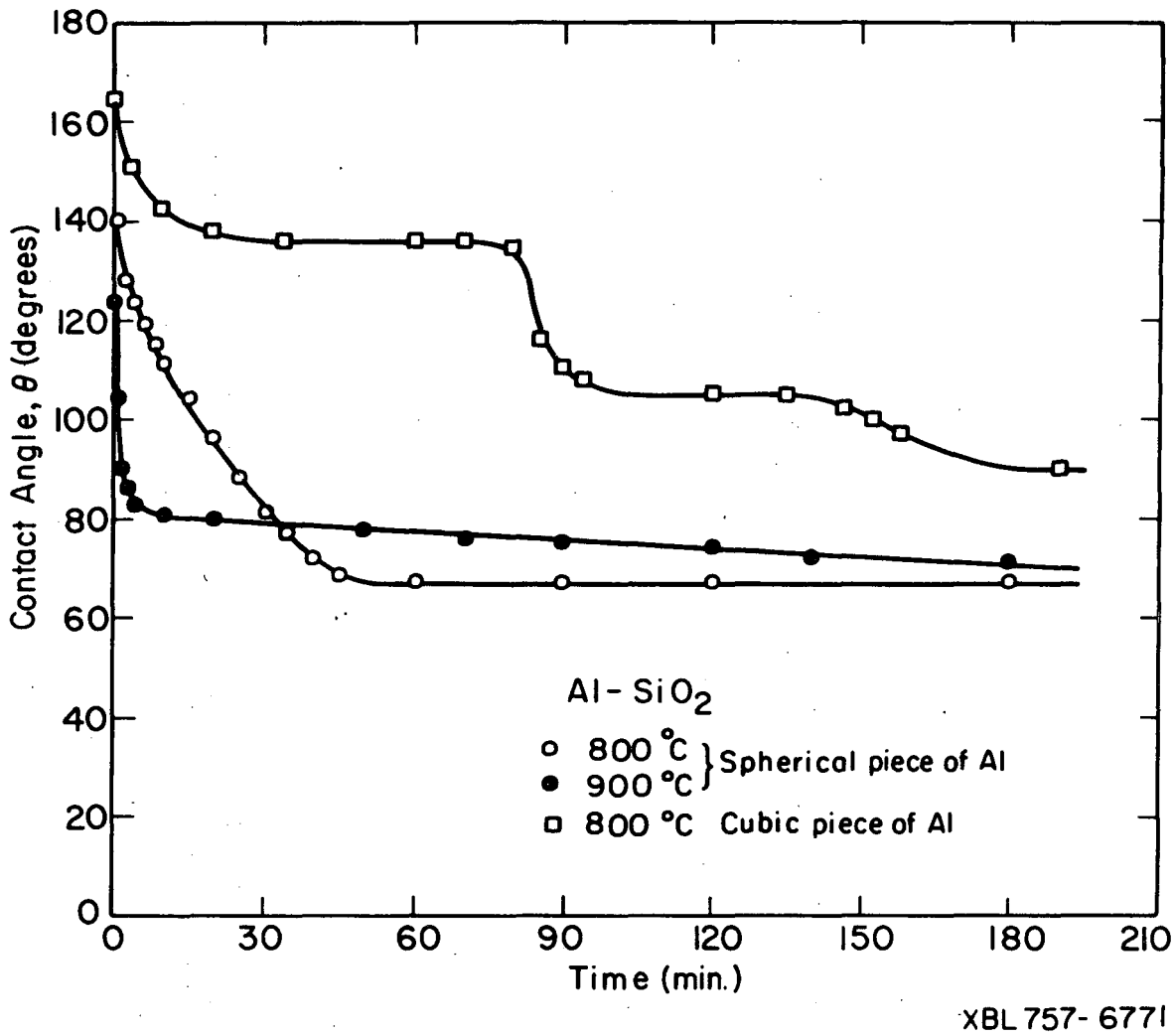

Fig. 4. Change in contact angle with time in the Al-SiO_2 system at 800°C and 900°C.

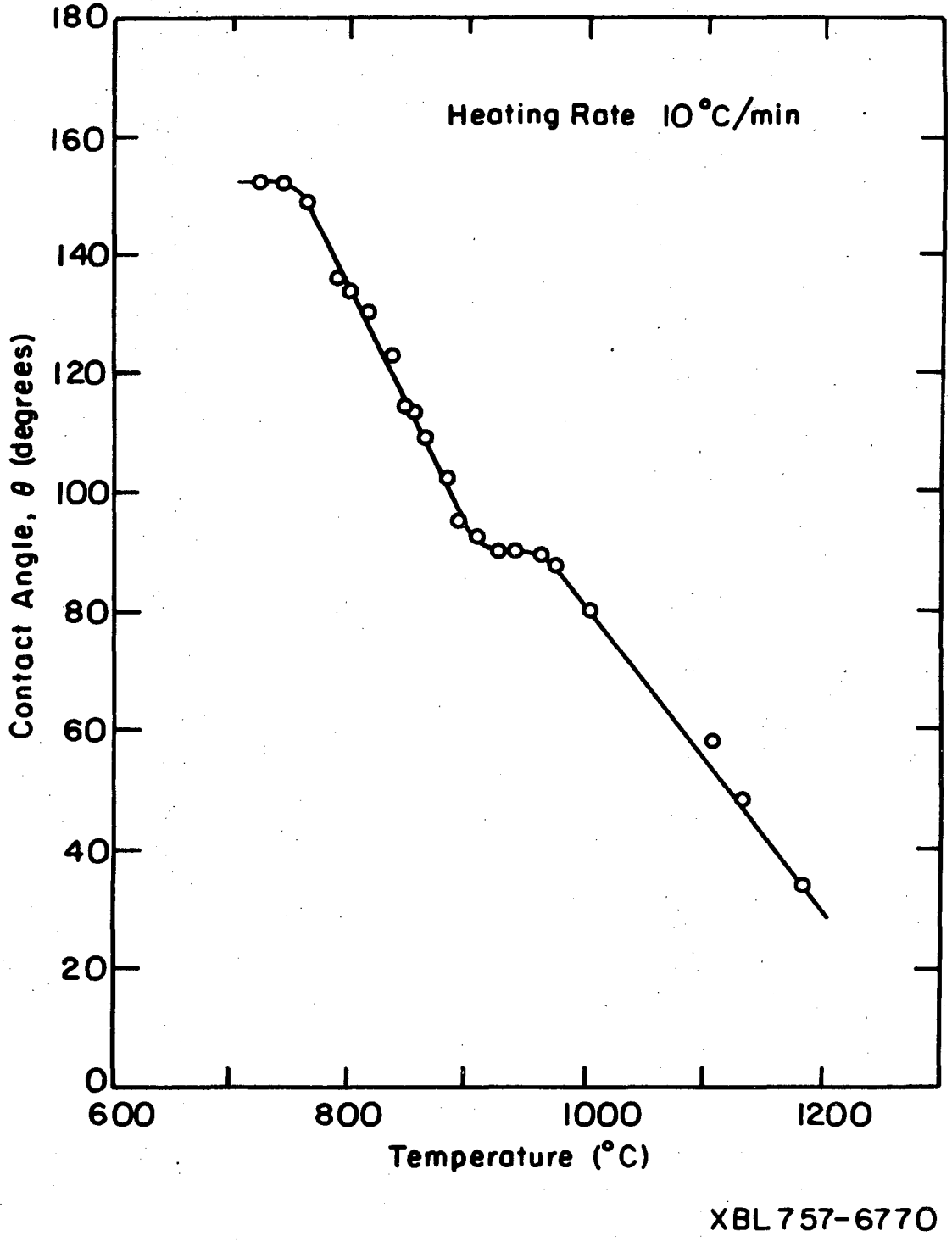

Fig. 5. Change in contact angle with temperature in the Al-SiO_2 system.

specimens perpendicular to the Al-SiO_2 interface after 17 minutes are shown in Fig. 6 and after 40 minutes in Fig. 7. The microstructure of the metal drop in the former shows Al and an eutectic mixture and in the latter, Si and an eutectic mixture. The 40 minute specimen showed a higher concentration of Si near the Al-reaction layer interface and near the periphery of the drop.

At 900°C, the growth rate of the reaction layer was always faster than the flow rate of molten Al. The reduction of the contact angle to about 80° occurred in about 10 minutes. The continued reduction of the contact angle was slow, taking about 3 hours to get down to 70°.

B. Reactions between Molten Aluminum and Fused Silica

The reactions at the liquid-solid interfaces involved a redox reaction with a replacement of Al in the drop with Si, as described above, and a replacement of Si in the substrate with Al. The reaction zone in the substrate was generally classified into three layers: I (adjoining the drop), II, and III (adjoining the unreacted SiO_2). The notation a indicates 900°C; b, 800°C; c, Al-Si alloy at 800°C; and d, 1000°C.

The composition of the reaction layers was analyzed with an electron microprobe. The line scanning technique, length of approximately 75 μm, was used to get the average composition at a given distance from the interface. Spot scanning was also used to analyze regions near boundaries. The results of composition analysis, after being corrected by computer* are shown for 800°C in Fig. 17 and for 900°C in Fig. 18. No

*Corrections were made for deadtime losses, background, absorption, characteristic fluorescence, back scatter losses, and ionization-penetration losses.

concentration gradients were detected in the reaction layers I adjoining the metal drop. Concentration gradients were present in the third layer III-a at 900°C. Analysis of layer II indicates irregularities suggesting the presence of several phases at temperature. The average composition of each reaction layer is shown in Table II.

Reaction products present at room temperature were analyzed by X-ray diffraction. The main reaction layer I-b at 800°C and the first layer I-a at 900°C after 1 hour of reaction were composed of θ-Al_2O_3, α-Al_2O_3, Al and Si. In the second layer II-a at 900°C, II-d at 1000°C in Al-SiO_2, and the main reaction layer II-c at 800°C in Si-saturated Al-SiO_2, α-Al_2O_3, Al and Si were detected. In the third layer III-d at 1000°C, θ-Al_2O_3, Al and Si were detected.

Selected micrographs of reaction layers between Al and SiO_2 and between Al-Si alloy and SiO_2 at different temperatures are shown in Fig. 8 to 16. Figure 8 and Fig. 10 show the microstructure of the layer I which adjoins the Al drop for the specimens at 800°C and 1000°C. Figure 11-a shows the microstructures of the three reaction layers I-d, II-d, III-d at 1000°C and Fig. 11-b shows the microstructure of the layer II-d at 1000°C. The morphologies of the reaction layers at 800°C and above 900°C are quite different. At 800°C, I-b is the dominant layer with a fine microstructure. The region with concentration variation near the fused silica probably corresponds to layers II and III above 900°C, although a distinct boundary could not be identified by an optical microscope. At 900°C and above, three layers are formed. Layer I has a similar microstructure to the layer I-b at 800°C. Layer II is very inhomogeneous and layer III has a fine microstructure. X-ray fluorescence

pictures of Al Kα, and Si Kα at 800°C are shown in Fig. 9 and at 900°C are shown in Figs. 12, 13 and 14. The Si precipitates in Al drop can be identified in Figs. 9 and 12. Al and Si distribution in layer I (Figs. 9, 12) and in layer III-a (Fig. 14) is fairly uniform. Figure 13 shows that the Si content in layer II-a is higher than I-a and III-a, and the distribution of Si is irregular. Figure 15 shows the microstructure of the reaction layer in the Si saturated Al (Al-28.3 wt% Si)-SiO_2 at 800°C. There is no layer equivalent to I and the main layer II-c which is in contact with the Al drop is very similar to II-a. The existence of layer III-c which has a microstructure that is identical to III-a is known from the X-ray fluorescence pictures in Fig. 16.

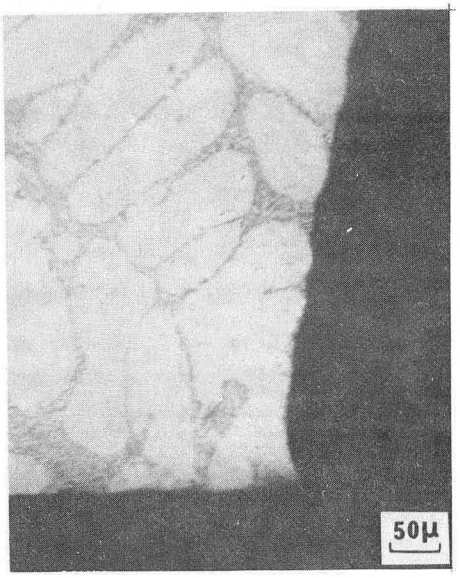

(a)

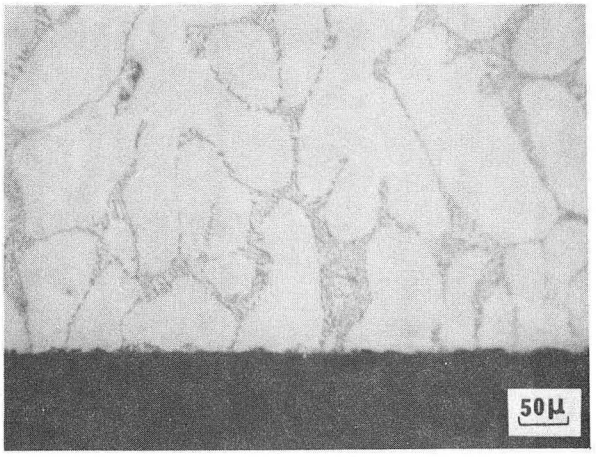

(b) XBB-757-5713

Fig. 6. Optical micrographs of Al drop after reaction with SiO_2 at 800°C for 17 min. Contact angle is 100°. (a) Micrograph of the edge of the drop which is beyond the reaction layer and in contact with unreacted SiO_2; the drop is Al interspersed with the Al-Si eutectic. (b) Micrograph of the inner part of the same specimen.

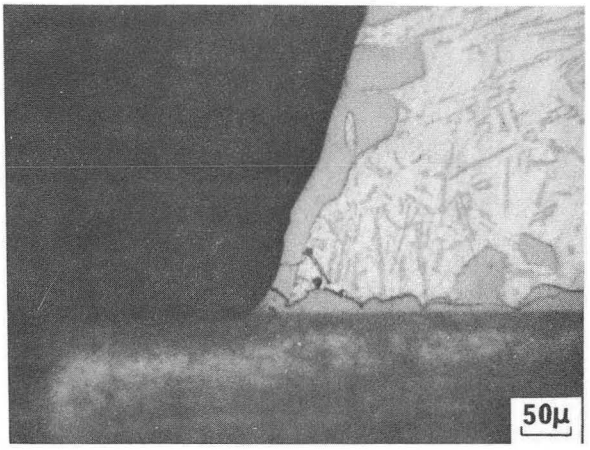

(a)

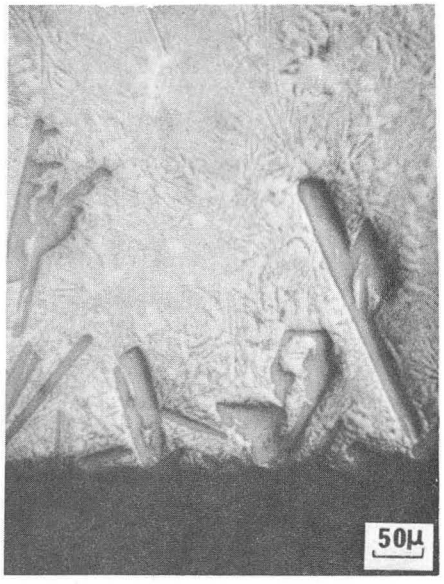

(b) XBB-757-5711

Fig. 7. Optical micrographs of Al drop after reaction with SiO_2 at 800° for 40 min. Contact angle is 70°. (a) Micrograph of the edge of the drop which lies within the reaction layer; the drop is Si interspersed with the Al-Si eutectic. (b) Micrograph of the inner part of the same specimen.

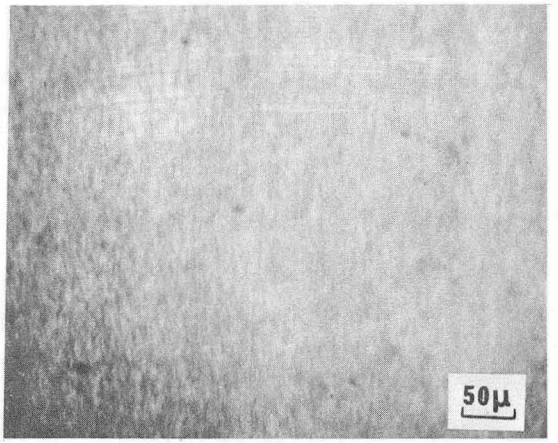

(a)

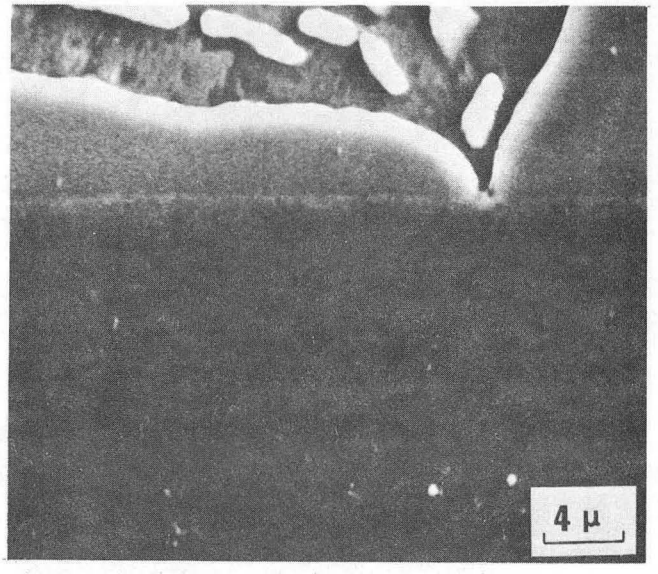

(b) XBB-757-5712

Fig. 8. (a) Optical micrograph of the first reaction layer (I-b) after reaction at 800°C for 1 hour. (b) Scanning electron micrograph of the Al-(I-b) interface region after reacting at 800°C for 1 hour.

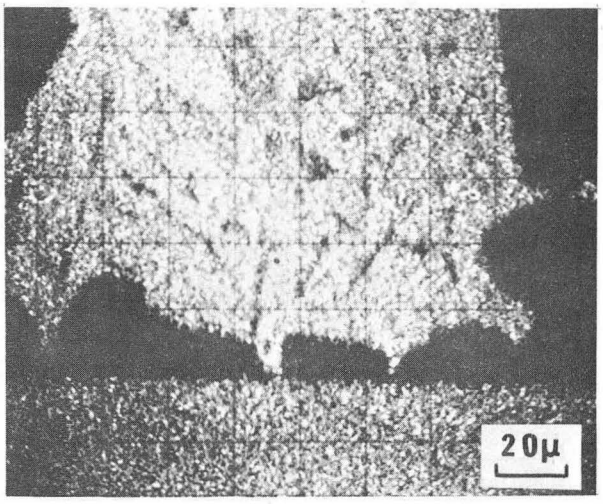

(a)

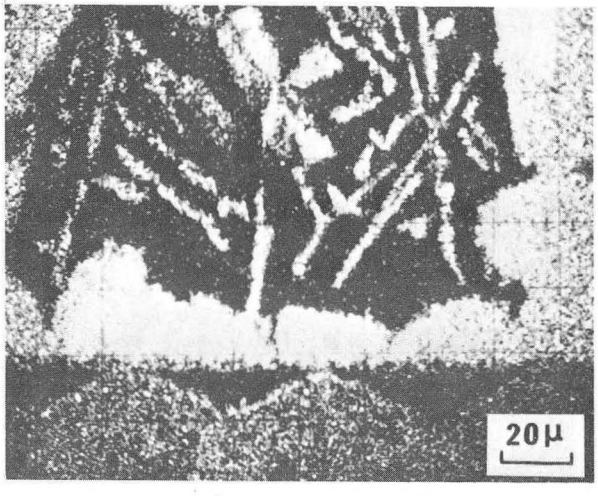

(b) XBB-757-5709

Fig. 9. X-ray fluorescence micrographs near the Al-(I-b) interface after reacting at 800°C for 1 hour. (a) Al-Kα (b) Si-Kα.

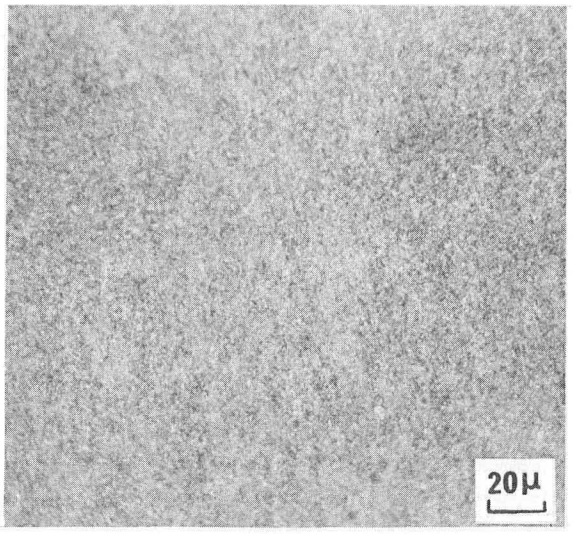

(a)

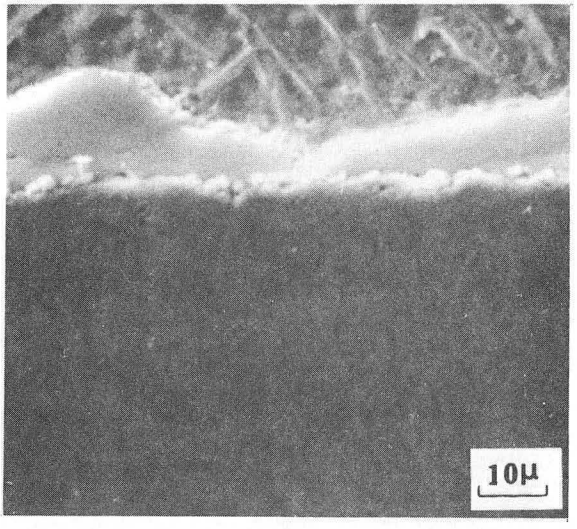

(b) XBB-758-6283

Fig. 10. (a) Optical micrograph of the first reaction layer (I-d) reacting at 1000°C for 1 hour.
(b) Scanning electron micrograph near the Al-(I-d) interface after reacting at 1000°C for 1 hour.

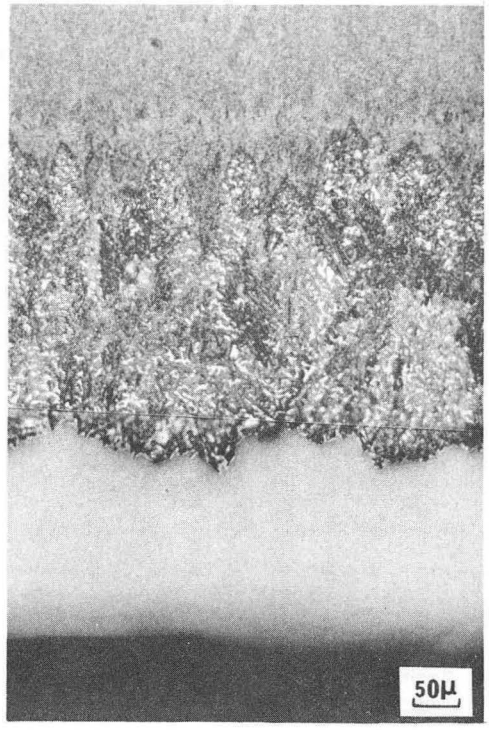

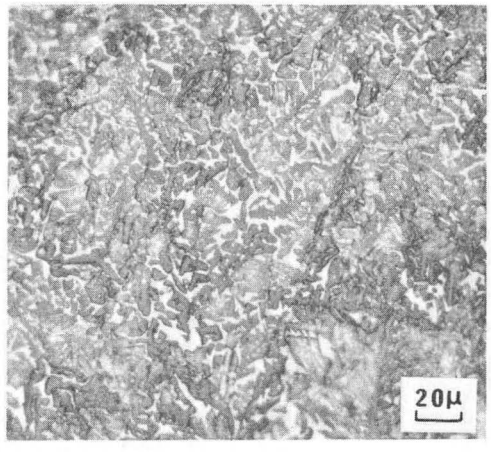

(b) XBB-758-6284

Fig. 11. (a) Optical micrograph of the first (I-d), second (II-d) and third (III-d) reaction layers after reacting at 1000°C for 1 hour.
(b) Optical micrograph of the second layer (II-d) after reacting at 1000°C for 1 hour.

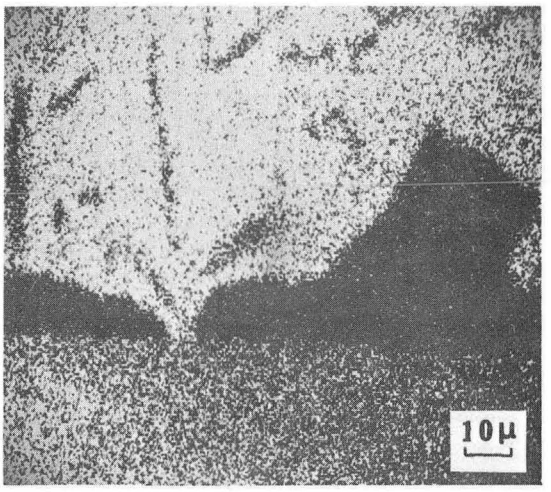

(a)

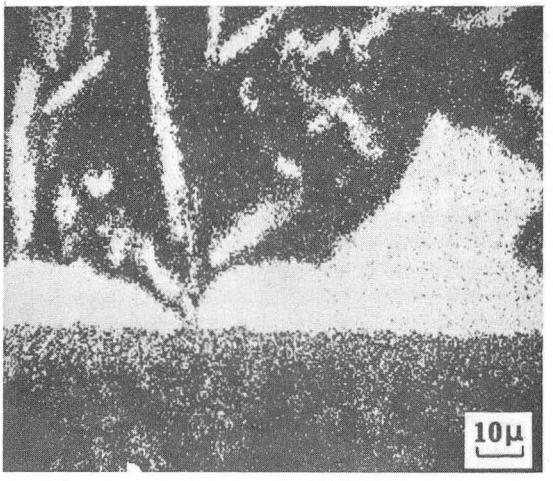

(b) XBB-757-5708

Fig. 12. X-ray fluorescence micrographs near the Al-(I-a) interface after reacting at 900°C for 1 hour. (a) Al-Kα (b) Si-Kα.

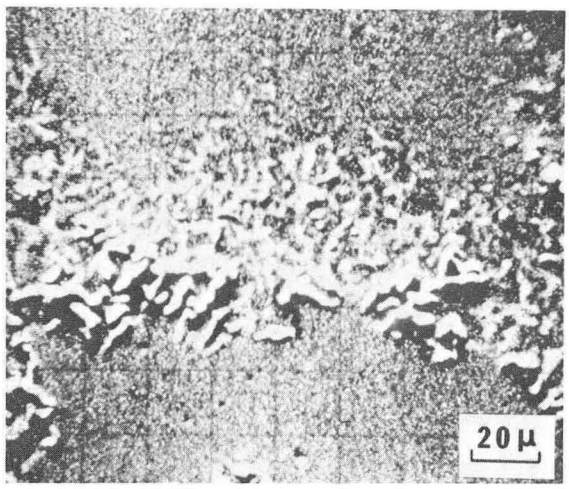

(a)

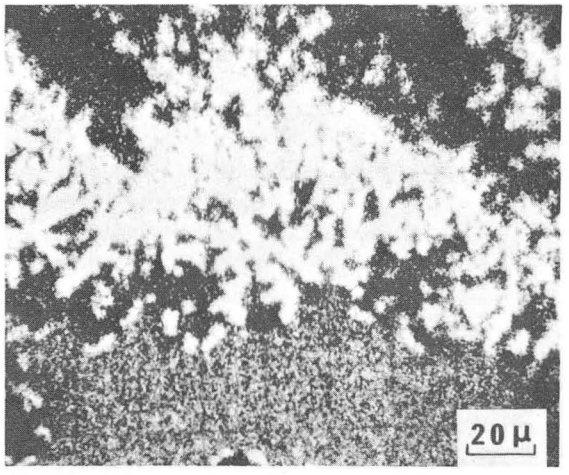

(b) XBB-757-5707

Fig. 13. X-ray fluorescence micrographs of the first (I-a), second (II-a) and third (III-a) layers after reacting at 900°C for 1 hour. (a) Al-Kα (b) Si-Kα.

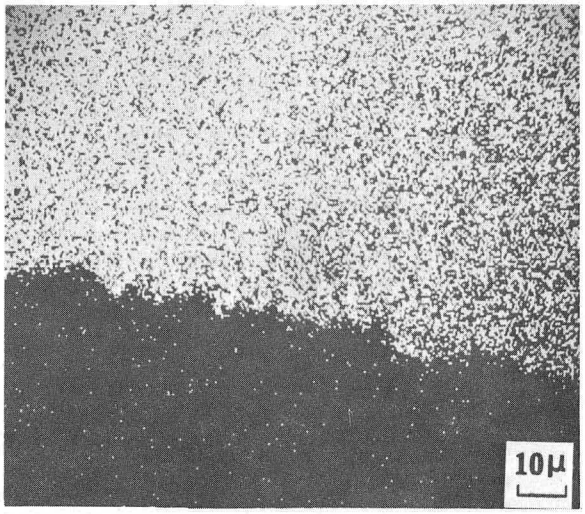

(a)

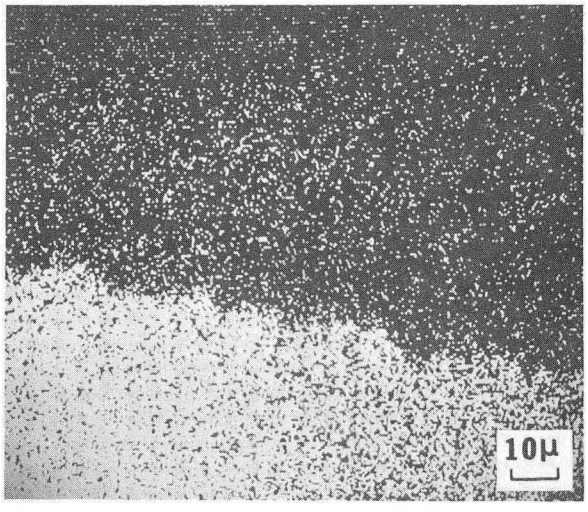

(b) XBB-757-5705

Fig. 14. X-ray fluorescence micrographs near the (III-a)-SiO_2 interface after reacting at 900°C for 1 hour. (a) Al-Kα (b) Si-Kα.

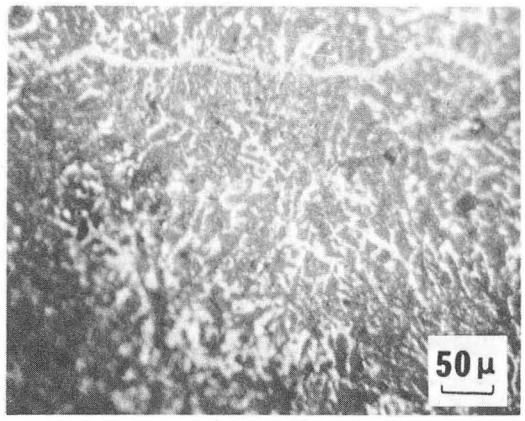

(a)

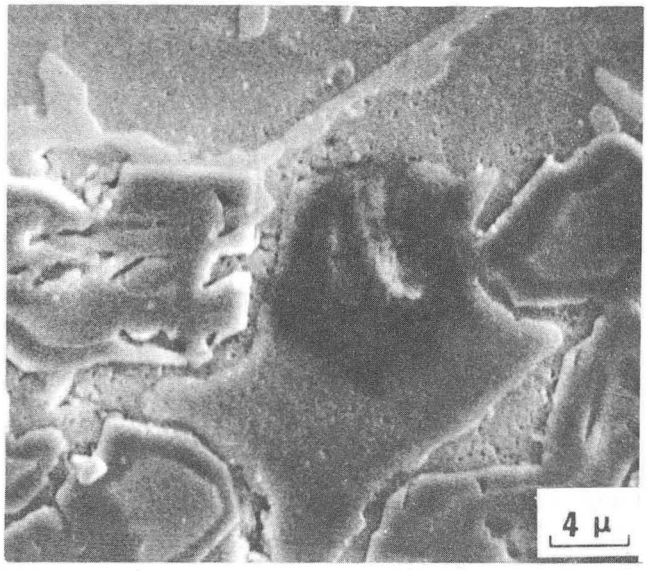

(b) XBB-757-5710

Fig. 15. (a) Optical micrograph of the reaction layer (II-c) in the Si saturated Al (Al-28.3 wt% Si)-SiO_2 system after reacting at 800°C for 24 hours.
(b) Scanning electron micrograph near the Al-(II-c) interface after reacting at 800°C for 24 hours.

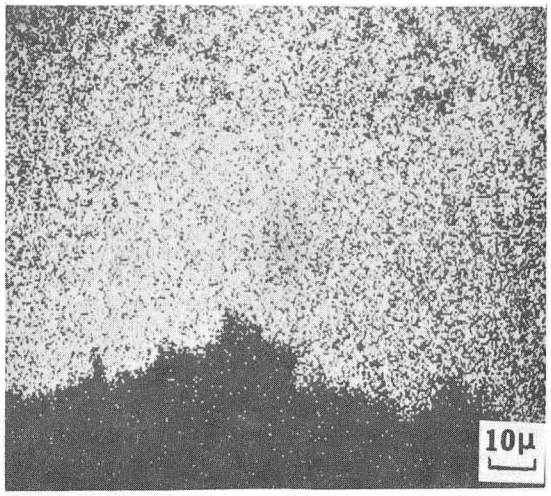

(a)

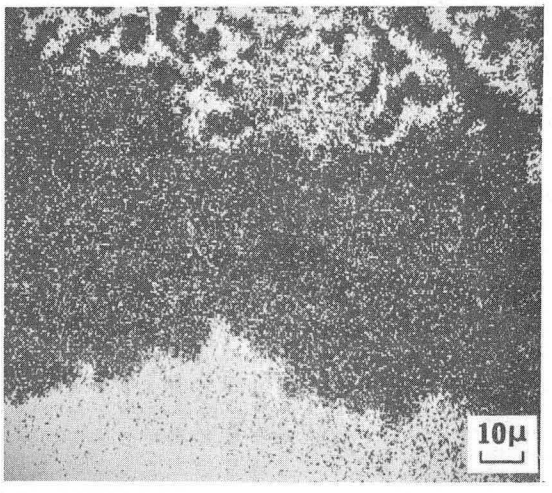

(b) XBB-757-5706

Fig. 16. X-ray fluorescence micrographs near the (III-c)-SiO_2 interface in the Si saturated Al(Al-28.3 wt% Si)-SiO_2 System. Two reaction layers (II-c and III-c) are recognized. (a) Al-Kα (b) Si-Kα.

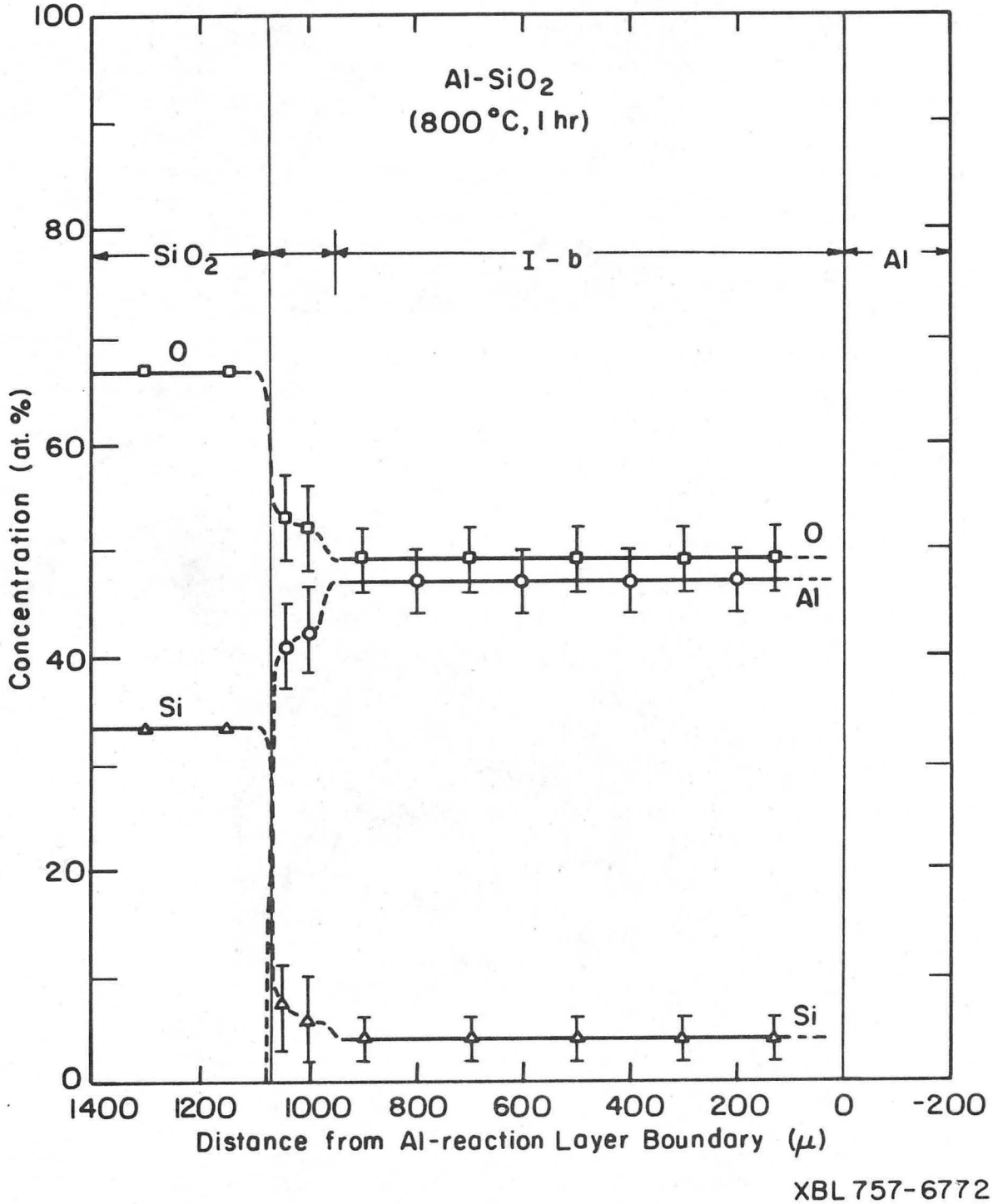

Fig. 17. Electron microprobe analysis of a cross-section in the Al-SiO_2 system reacted at 800°C for 1 hour.

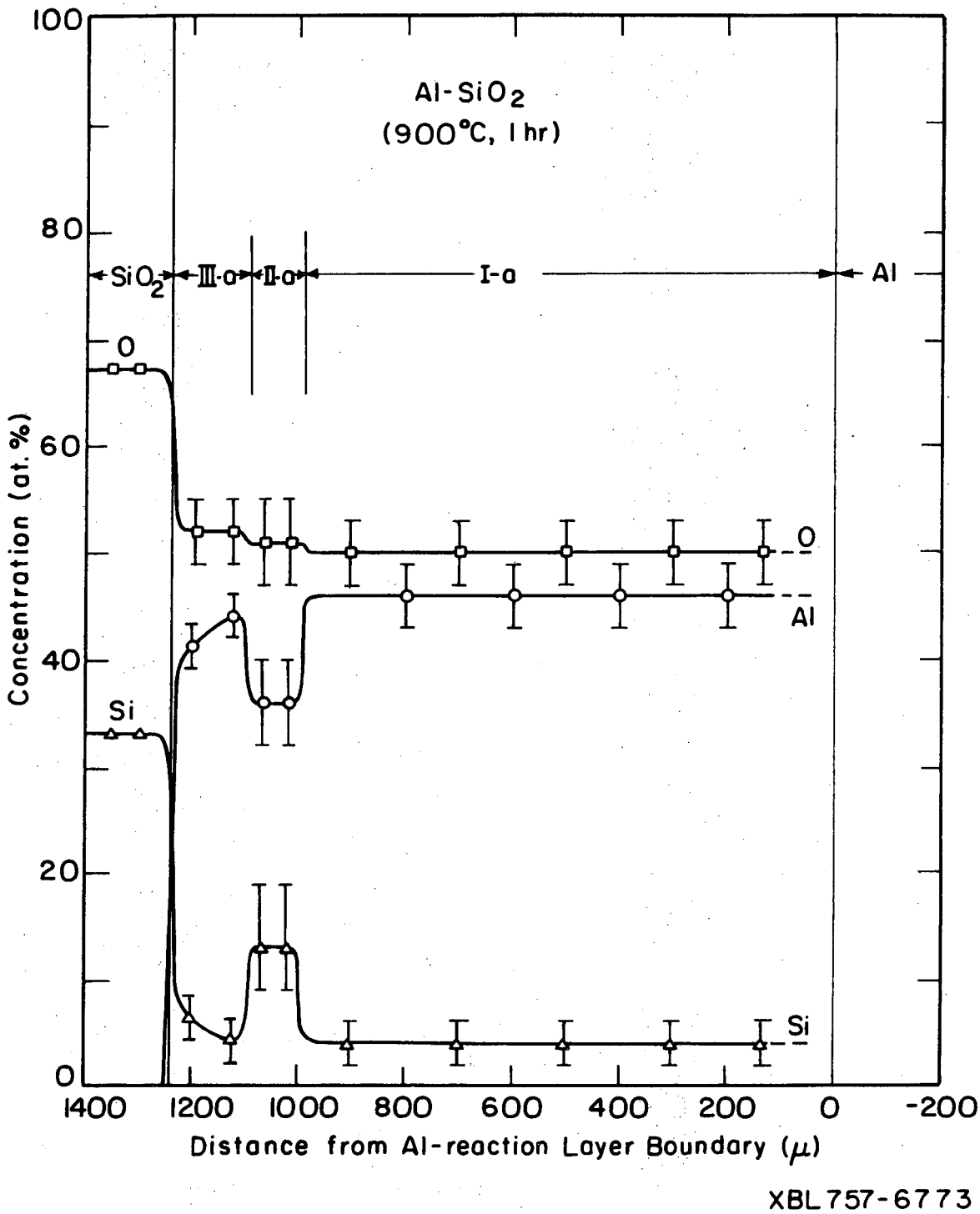

Fig. 18. Electron microprobe analysis of a cross-section in the Al-SiO_2 system reacted at 900°C for 1 hour.

Table II. Average Compositions of Several Reaction Layers.

Layer	Temp. (°C)	Time (min.)	Al (at. %)	O* (at. %)	Si (at. %)
1st (I-b)	800	8	47 ± 3	51 ± 3	2 ± 1
1st (I-b)	800	60	47 ± 3	49 ± 3	4 ± 2
1st (I-a)	900	60	46 ± 3	50 ± 3	4 ± 2
2nd (II-a)	900	60	36 ± 4	51 ± 4	13 ± 4
3rd (III-a)	900	60	44—40	52 ± 3	4—8

($\bar{X} \pm 2 \times$ Standard Deviation)

* O at. % = 100 - (Al at. % + Si at. %)

XBL 757-6769

V. DISCUSSION

A. Wetting Behavior in the Al-SiO_2 System

The contact angle in a solid-liquid-vapor system under chemical equilibrium is determined by the relative magnitudes of the three interfacial tensions. Yin[34] showed that the rate of increase of the solid-liquid interfacial area, until it reaches the static or steady state under chemical equilibrium conditions, is linear and only a function of viscosity, surface tension and initial contact angle.

If there is a reaction at the solid-liquid interface, the reduction of $\gamma_{s\ell}$ due to the contribution of the free energy of the reaction $(-)\Delta g^{s\ell}$ must be considered. Since the reaction between Al and SiO_2 is extensive, the contribution of the free energy of reaction $(-)\Delta g^{s\ell}$ to the initial decrease of the contact angle must be significant.

The change of $\gamma_{\ell v}$ and of viscosity η due to the dissolution of Si into Al liquid also have to be taken into account. The surface tension of Al at 800°C is 860 dyne/cm and at 900°C, 850 dyne/cm.[35] The extrapolated value of the surface tension of Al to 1450°C is 810 dyne/cm. The surface tension of Si (m.p. 1410°C) at 1450°C is 730 dyne/cm.[36] It is known that the component which has a lower surface tension is present at a higher concentration in the surface compared to the bulk ideal mixture in a binary liquid. As shown in Fig. 7, the Si concentration at the surface of the drop is higher, indicating that the dissolution of Si lowers the surface tension of the aluminum liquid. The viscosity η for pure Al is 1 cP and that for Al-28 wt% Si is 0.8 cP at 800°C.[37] The viscosity of Al itself and its change with Si composition is so small

that the effect of the change of viscosity is considered to be negligible. Therefore, the first decrease of contact angle is considered to be mainly due to the contribution of the free energy of the reaction $(-)\Delta g^{s\ell}$ and to the decrease of the surface tension of the liquid.

In the absence of a reaction the contact angle would be obtuse since γ_{sv} of fused SiO_2 is $\sim$300 dyne/cm which is smaller than $\gamma_{\ell v}$. At 800°C as the contact angle decreases to 90° the periphery of the drop keeps in contact with the unreacted SiO_2 surface. As the reaction proceeds, the Si concentration at the solid-liquid interface increases causing a reduction in the driving force for the reaction which results in the reduction of the flow rate of the liquid. At the contact angle of $\sim$90°, the reaction layer exceeds the periphery of the drop as observed experimentally at 800°C. At this point the periphery of the drop remains in contact with layer I with which reaction continues but with a smaller $(-)\Delta g^{s\ell}$.

At 900°C, the thickness of layer I was reduced, and layers II and III increased in thickness. As the contact angle dropped below 90° the periphery of the drop was in contact with layer II. The difference of the wetting behavior at 800°C and at 900°C (Fig. 4) is due to the faster rate of the reaction at the higher temperature and to the difference of the nature of the reaction as indicated by the faster growth rate of layers II and III at the higher temperature.

Around 800°C, the effect of layer I is predominant, and above 900°C, the effect of layer II becomes predominant. This transition of the wetting behavior is reflected in the change of the slope of the temperature dependence of the contact angle and the arrest at $\sim$900°C (Fig. 5).

B. The Reaction Mechanism in the Al-SiO_2 System

The following reaction mechanism is proposed based on the experimental results. The related phenomena will be discussed.

1. The Diffusion Model

It is proposed that the reaction proceed by counterdiffusion of aluminum ions and silicon ions through the reaction layers in which the oxygen content remains constant. The proposed mechanisms are schematically shown in Fig. 19. The following reactions at the interfaces are indicated:

(a) At the Al liquid-layer I interface

$$Al = Al^{+} + e^{-}$$

$$Al = Al^{++} + 2e^{-}$$

$$Si^{++} + 2e^{-} = Si$$

(b) At the layer I-layer II interface

$$Al^{+} + Al^{3+} = 2Al^{++}$$

(c) At layer III-SiO_2 interface

$$Al^{++} = Al^{3+} + e^{-}$$

$$Si^{4+} + 2e^{-} = Si^{++}$$

Layer I has a constant composition and is assumed to be essentially AlO with SiO and some Al_2O in solid solution. It is postulated that solid AlO is stabilized by this solid solution. If the microprobe analysis for layer I is taken as 48 at% Al, 48 at% O and 4 at% Si (Table II), the oxide content can be calculated as 84% AlO, 8% Al_2O and 8% SiO. X-ray diffraction analysis at room temperature indicates the presence of θ-Al_2O_3, α-Al_2O_3, Al and Si. θ-Al_2O_3 has a monoclinic cell

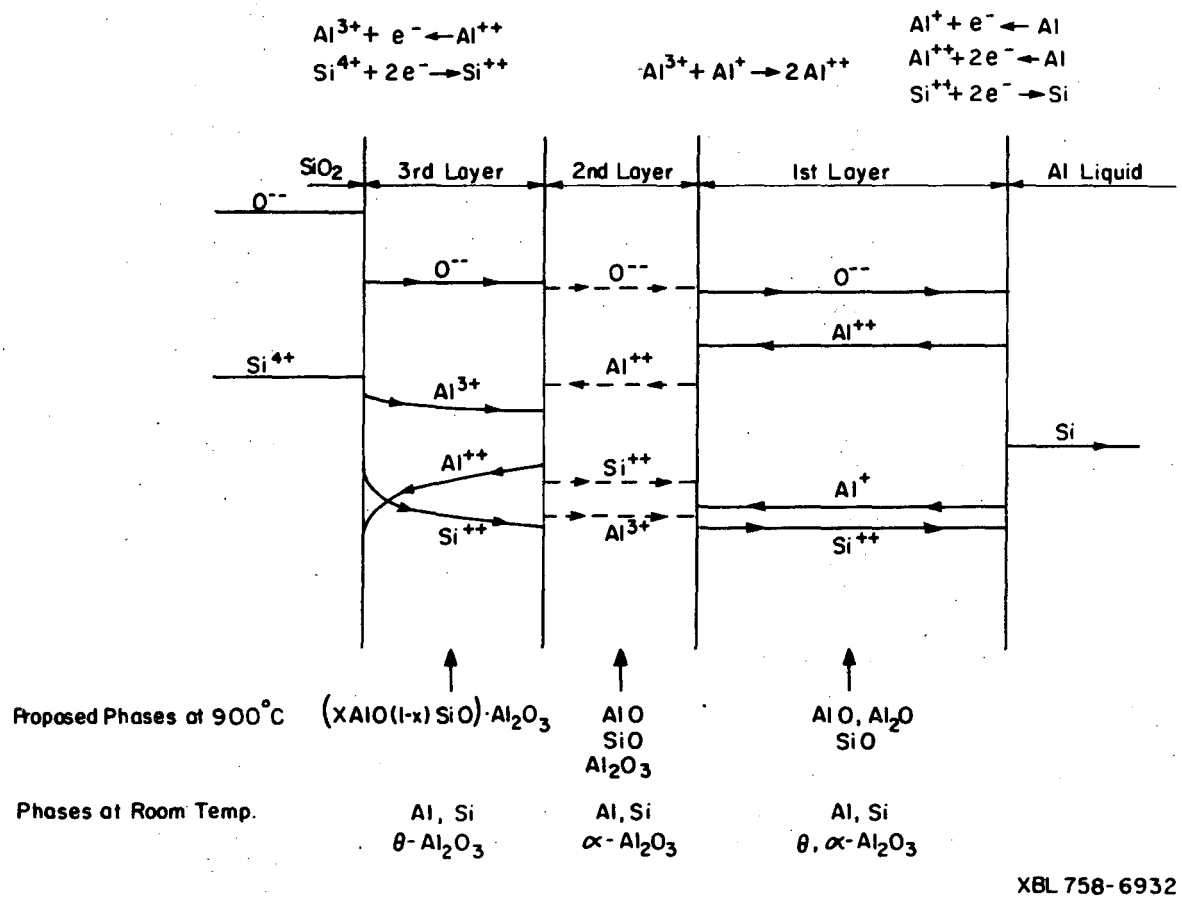

Fig. 19. Schematic diagram of the proposed reaction mechanism in the Al-SiO_2 system.

and the structure can be described as a deformed spinel type with aluminum ions occupying both octahedral and tetrahedral positions. The dissociation of AlO and Al_2O on cooling is likely to be responsible for the formation of θ-Al_2O_3 besides α-Al_2O_3. The fine microstructure of the reaction layer I (Figs. 8 and 10) is considered to be due to the presence of a homogeneous phase at temperature which dissociates to a fine-grained structure on cooling.

Layer III (Fig. 14) is assumed to be a spinel type structure $(XAlO(1-X)SiO)Al_2O_3$ through which Al^{++} and Si^{++} counterdiffuse. If the composition in layer III is 39 at% Al, 4 at% Si, and 57 at% O (Table II) the resulting oxide composition becomes $(0.73AlO\ 0.27SiO)Al_2O_3$. The spinel type structure at temperature is considered to dissociate to θ-Al_2O_3, Al and Si.

Layer II-a is assumed to be a two-phase region composed of a AlO and SiO solid solution and an Al_2O_3 rich phase at temperature. With an excess of Al^{3+} and a limited amount of Al^{+} from the layer I-a interface α-Al_2O_3 is precipitated in two phase matrix. In a three component diffusion couple, two-phase region can be expected. The precipitates in the two-phase matrix should not disturb the diffusion paths. Tressler et al.[33] observed precipitates of $(Ti,Al)_2O_3$ in the Al_2O_3-TiO interfacial region. α-Al_2O_3 precipitates are likely to provide the nucleation sites of α-Al_2O_3 when AlO dissociates to Al and Al_2O_3 on cooling. Also, it is likely that the existence of large amounts of SiO which release oxygen on dissociation during cooling enhances the formation of α-Al_2O_3. On cooling AlO and SiO are expected to dissociate independently as follows:

$$3AlO = Al + Al_2O_3$$

$$2SiO = Si + SiO_2$$

When they coexist, the following reaction is expected:

$$5AlO + SiO = Al + 2Al_2O_3 + Si$$

a composition of 68% AlO, 28% SiO and 4% Al_2O_3 is consistent with the microprobe analysis (36 at% Al, 51 at% O, 13 at% Si) (Table II).

The thickness of each reaction layer is determined by its relative growth rate. The first layer grows when the Al is not saturated with Si (as described for layer I-b). When the Al becomes saturated with Si the growth rate of the second layer is accelerated. In the case of Si-saturated Al-SiO_2 reaction at 800°C, the first layer is not formed, and a thick second layer (II-c) and a thin third layer (III-c) are formed (Figs. 15 and 16). In the case of Al-SiO_2 reaction at 800°C, the growth rate of the second layer is so slow that the existence of that cannot be detected.

2. Possibility of Molten Aluminum Penetration into the Reaction Layers

A possible alternative explanation for the existence of significant amounts of aluminum in the reaction layers is the penetration of molten aluminum into the reaction layers. If the reaction between Al and SiO_2 is carried to completion according to Eq. (1), 3 moles of SiO_2 are replaced by 2 moles of Al_2O_3. Since the volume of 3 moles of SiO_2 (density 2.22 g/cm^3) is 81.1 cm^3 and that of 2 moles of Al_2O_3 (assume α-Al_2O_3, density 3.9 g/cm^3) is 52.3 cm^3, this replacement causes a porous Al_2O_3 layer into which the penetration of molten aluminum and the diffusion of Si through the Al to the liquid drop may be possible. In spite of this possibility, this mechanism is unlikely because of the following reasons.

(a) Observation of the microstructures of the first layer (I-a, I-d) with the electron scanning microscope (Fig. 8, Fig. 10) showed no evidence of open pores through which molten aluminum could penetrate. Since the microstructure of the first layer is so fine-grained, it is more likely that this layer was homogeneous at the experimental temperature and dissociated during cooling.

(b) The third layer (III-a) showed a concentration gradient (Fig. 18). The existence of the third layer can only be explained by assuming the interdiffusion of Al^{++} and Si^{++}. Therefore, even if the liquid penetration is possible, it should be limited up to the third layer. This assumption, however, cannot explain how the first layer and the second layer are formed. If the reaction at the interface of the second layer-third layer is

$$Al = Al^{++} + 2e^{-}$$

$$Si^{++} + 2e^{-} = Si$$

and the reaction at the third layer-SiO_2 interface is

$$Al^{++} = Al^{3+} + e^{-}$$

$$Si^{4+} + 2e^{-} - Si^{2+},$$

there is no reason to form the first and second layer.

VI. CONCLUSION

From the studies on reactions and wetting behavior in the molten aluminum-fused silica system, the following conclusions are obtained.

(a) The initial contact angle decrease of molten aluminum on fused silica is mainly due to the contribution of the free energy of the reaction to the solid-liquid interfacial tension and the change of the surface tension of the Al liquid, $\gamma_{\ell v}$, because of enrichment with Si.

(b) A reaction mechanism for the Al-SiO_2 reaction is proposed. The reaction proceeds by counterdiffusion of Al ions and Si ions through the reaction layer.

(c) In the first reaction layer, formed when the Al liquid is unsaturated with Si, the existence of AlO stabilized by the formation of solid solution with SiO and Al_2O is postulated at temperature; on cooling to room temperature it dissociated to form θ- and α-Al_2O_3, Al, and Si. In the third layer, the formation of the spinel type structure (XAlO(1-X) SiO $\cdot Al_2O_3$) is assumed; this reaction is accelerated when the Al liquid becomes saturated with Si. On cooling it dissociates to form θ-Al_2O_3, Al and Si.

(d) To fully understand the Al-SiO_2 reactions, knowledge of the phase diagram of the Al-Si-O system is required. Studies of stabilities of aluminum and silicon suboxides with solid solution are also necessary.

ACKNOWLEDGMENT

The author wishes to express his sincere thanks to Professor Joseph A. Pask for his continuous guidance and instructions during this investigation. Particular thanks are expressed to Professor Richard M. Fulrath for his helpful suggestions and encouragement at all times.

The technical assistance of George Georgakopoulos and Richard Lindberg for using the electron microprobe, of Kelly Radmilovic for typing is greatly appreciated. Discussions with students in the ceramic division were very helpful and acknowledged.

The financial support for the research by Kanebo, Ltd. is acknowledged.

Finally, the author wishes to express his thanks to his parents, Mr. and Mrs. Y. Marumo and to his whole family for their continuous encouragement at all times.

REFERENCES

1. I. A. Aksay, C. E. Hoge and J. A. Pask, J. Phys. Chem., 78 (12) 1178 (1974).
2. A. E. Standage and M. S. Gani, J. Am. Ceram. Soc., 50 (2) 101 (1967).
3. R. E. Johnson, Jr., J. Phys. Chem., 63 1655 (1959).
4. K. J. Brondyke, J. Am. Ceram. Soc., 36 (5) 171 (1953).
5. D. Cratchley and A. A. Baker, Ceramic Bulletin, 46 (2) 191 (1967).
6. K. Prabriputaloong and M. R. Piggott, J. Am. Ceram. Soc., 56 (4) 184 (1973).
7. K. Prabriputaloong and M. R. Piggott, J. Am. Ceram. Soc., 56 (4) 177 (1973).
8. K. Prabriputaloong and M. R. Piggott, J. Electrochem. Soc.: Solid State Science and Technology, 121 (3) 430 (1974).
9. L. Brewer and A. W. Searcy, J. Am. Chem. Soc., 73 (11) 5308 (1951).
10. E. Baur and R. Brunner, Z. Elektrochem., 40 (8) 154 (1934).
11. E. J. Kohlmeyer and S. Lundquist, Z. Anorg. Allgem. Chem., 260 208 (1949).
12. L. M. Foster, G. Long and M. S. Hunter, J. Am. Ceram. Soc., 39 (1) 1 (1956).
13. H. Yanagida and F. A. Kröger, J. Am. Ceram. Soc., 51 (12) 700 (1968).
14. M. Hoch and H. L. Johnston, J. Am. Chem. Soc., 76 (9) 2560 (1954).
15. J. M. Charig and D. K. Skinner, "Proceedings of the Conference on the Structure and Chemistry of Solid Surface," G. A. Somorjai, Ed. John Wiley and Sons, New York, N.Y., 1963, P34.
16. C. C. Chang, ibid., P77.

17. T. M. French and G. A. Somorjai, J. Phys. Chem., 74 (12) 2489 (1970).

18. J. J. Brennan and J. A. Pask, J. Am. Ceram. Soc., 51 (10) 569 (1968).

19. S. Yamaguchi, Werkstoffe und Korrosion, 25 (5) 325 (1974).

20. For Example, P. G. Saper, Phys. Rev., 42 498 (1932).

21. H. Schäfer and R. Hörnle, Z. Anorg. Allg. Chem., 263 261 (1950).

22. L. Brewer and D. Mastick, J. Chem. Phys., 19 834 (1951).

23. O. Kubaschewski, E. L. Evans and C. B. Alcock, Metallurgical Thermochemistry, 4th ed., Pergamon Press, New York (1967).

24. L. Brewer and R. K. Edwards, J. Phys. Chem., 58 351 (1954).

25. P. V. Gel'd and M. I. Kochev, Zhur. Pliklad. Khim., 21 1249 (1948).

26. G. Grube and H. Seidel, Z. Electrochem., 53 339, 341 (1949).

27. H. von Wartenberg, Z. Electrochem., 53 343 (1949).

28. M. Hoch and H. L. Johnson, J. Am. Chem. Soc., 75 5224 (1953).

29. S. Geller and C. D. Thurmond, J. Am. Chem. Soc., 77 5285 (1955).

30. H. N. Potter, Trans. Am. Electrochem. Soc., 12 191, 215, 223 (1907).

31. L. Brewer and F. T. Greene, J. Phys. Chem. Solid, 2 286 (1957).

32. C. B. Alcock, Trans. Brit. Ceram. Soc., 60 (2) 147 (1961).

33. R. E. Tressler, T. L. Moore and R. L. Crane, J. Mater. Sci., 8 151 (1973).

34. T. P. Yin, J. Phys. Chem., 73 (7) 2413 (1969).

35. S. H. Overbury, P. A. Bertrand and G. A. Somorjai, "The Surface Composition of Binary Systems. Prediction of Surface Phase Diagrams of Solid Solutions," Chem. Rev., to be published.

36. M. Hunenik, Jr. and W. D. Kingery, J. Am. Ceram. Soc., 37 (1) 18 (1954).

37. V. M. Glazov and A. A. Vertman, "Structure and Properties of Liquid Metals," A. M. Samarin, ed., Moscow, Academy of Science, USSR, Baikov's Institute of Metallurgy, 1960, P.121.

TECHNICAL INFORMATION DIVISION
LAWRENCE BERKELEY LABORATORY
UNIVERSITY OF CALIFORNIA
BERKELEY, CALIFORNIA 94720